Electronic Supplementary Information

Side-Chain Engineering of Wide-Bandgap Polymers Based on Benzo[1,2-b:4,5-b′]dithiophene and [2,2′-bithiophene]-4,4′-Dicarboxylate for Fullerene-Free Organic Solar Cells

Qi Wang,[a] Miaomiao Li,*[a,b] Ying Sui,[a] Zhongli Wang,[a] Ziqi Liang[a] and Yanhou Geng*[a,b]

[a]School of Materials Science and Engineering, Tianjin University, Tianjin 300072, P. R. China.

[b]Tianjin Key Laboratory of Molecular Optoelectronic Science, Tianjin University, and Collaborative Innovation Center of Chemical Science and Engineering (Tianjin), Tianjin 300072, P. R. China.

Instruments

^{1}H NMR and ^{13}C NMR spectra were measured by a Bruker AV 400-MHz spectrometer in $CDCl_3$ or 1,1,2,2-$C_2D_2Cl_4$ using tetramethylsilane (TMS) as internal standard. Gas chromatography-mass spectra (GC-MS) were recorded on a Shimadzu/GCMS-QP2010 SE mass spectrometer. Matrix-assisted laser desorption ionization time-of-flight (MALDI-TOF) mass spectra were recorded on a Bruker/AutoflexIII Smartbean MALDI mass spectrometer with 2-[(2*E*)-3- (4-*tert*-buthylphenyl)-2-methylprop-2-enylidene]malononitrile (DCTB) as the matrix in a reflection mode. Elemental analysis was measured by a FlashEA1112 elemental analyzer. Gel permeation chromatography (GPC) analysis of polymers was conducted on a PL-GPC 220 system with monodisperse polystyrene as standard and 1,2,4-trichlorobenzene as eluent at 150 °C. Thermogravimetric analysis (TGA) was conducted on Perkin-Elmer TGA-7 at a heating rate of 10 ºC/min under N_2 and differential scanning calorimetry (DSC) was performed by a Perkin-Elmer DSC7 thermal analyzer with a heating/cooling rate of ±10 °C/min under N_2. UV-*vis*-NIR absorption spectra were obtained on a Shimadzu UV3600 Plus Spectrometer. Cyclic voltamogram (CV) measurements were carried out on a CHI660 electrochemical analyzer with a three-electrode cell at a scan rate of 100 mV/s. A glassy carbon electrode (diameter of 1 cm), a platinum wire and a saturated calomel electrode (SCE) were used as working electrode, counter electrode and reference electrode, respectively. Tetrabutylammonium hexafluorophosphate (NBu_4PF_6, 0.1M) in anhydrous acetonitrile was used as the supporting electrolyte. The potential was calibrated by ferrocene/ferrocenium (Fc/Fc^+), and the HOMO/LUMO energy levels were estimated by the equations: $E_{\mathrm{HOMO}} = -(4.80 + E_{onset}^{ox})$ eV, $E_{\mathrm{LUMO}} = -(4.80 + E_{onset}^{re})$ eV, in which E_{onset}^{ox} and E_{onset}^{re} are oxidation and reduction onsets versus the half potential of Fc/Fc^+, respectively. X-ray diffraction (XRD) was conducted on a Rigaku Smart Lab with CuKα source (λ = 1.54056 Å). Atomic force microscopy (AFM)

images were recorded in tapping mode on a Bruker MutiMode 8 atomic force microscope.

Fabrication and characterization of PSC devices

PSC devices with a device architecture of glass/ITO/PEDOT:PSS (30 nm)/active layer /PDINO (10 nm)/Al (100 nm) were fabricated. ITO was cleaned ultrasonically with detergent, deionized water, acetone and isopropanol for 15 min, successively. The dried ITO was treated with UV-ozone for 25 min, and then solution of PEDOT:PSS (Baytron PVP Al 4083) was spin-coated on the surface. The ITO was dried by baking in an oven at 150 ^{o}C for 20 min. A chlorobenzene solution (total concentration: 18mg/mL) of donor:acceptor blend was subsequently spin-coated on the PEDOT:PSS layer to form a photosensitive layer (ca.~100 nm thick), followed with thermal annealing for 10 mins. The active layer thickness was measured using a Dektak150 profilometer. The PDINO in methanol solution was deposited on the active layer to give a interfacial layer. Aluminum top electrode (ca. 100 nm) was subsequently deposited on the PDINO layer under high vacuum ($< 1.5 \times 10^{-4}$ Pa). The effective area of each cell is 4 mm^2, as defined by masks for the solar cell devices. Keithley 2400 source meter was used to measure *J-V* curves under 100 mW cm^{-2} AM 1.5G simulated solar light illumination provided by a Solar Simulator (SS-F5-3A, Enli Technology Co. Ltd) calibrated with a standard photovoltaic cell equipped with a KG5 filter in a glove box. EQE curves were detected on a solar cell spectral response measurement system (QE-R, Enli Technology Co. Ltd).

Fabrication and characterization of SCLC devices

Hole-only devices with a device architecture of glass/ITO/PEDOT:PSS (30 nm)/active layer or polymer film (~100 nm)/Au (100 nm) and electron-only devices with a device architecture of glass/ZnO (30 nm)/ active layer (~100 nm)/Al (100 nm) were fabricated. The devices were measured using Keithley 2400 source meter in a glove box under dark. The hole and electron mobilities were extracted by fitting the

current density-voltage curves using SCLC method. The *J-V* curves of the devices were plotted as $J^{0.5}$ versus V using equation:

$$J = \frac{9}{8}\varepsilon_0\varepsilon_r\mu\frac{V^2}{L^3}$$

where J is the current density, L is the film thickness of the active layer, μ is the hole or electron mobility, ε_r is the relative dielectric constant of the transport medium, ε_0 is the permittivity of free space (8.85×10^{-12} F m^{-1}), V (= V_{appl} - V_{bi}) is the internal voltage in the device, where V_{appl} is the applied voltage to the device and V_{bi} is the built-in voltage due to the relative work function difference of the two electrodes.

Supplementary data

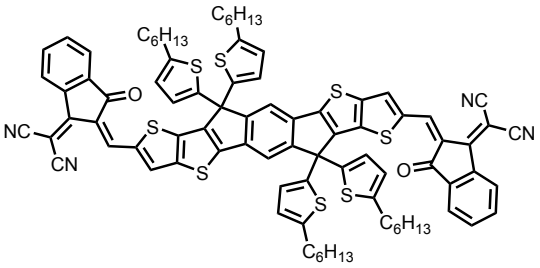

Fig. S1 Chemical structure of ITIC-Th.

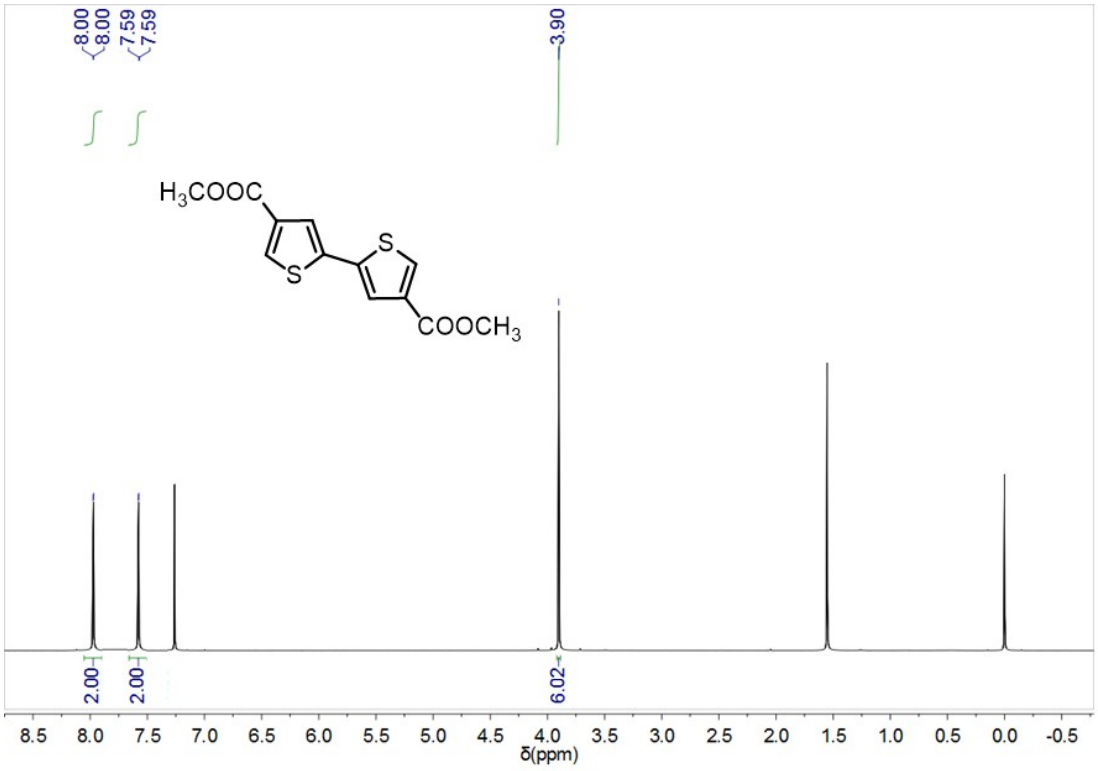

Fig. S2 ^{1}H NMR spectrum of compound **2a**.

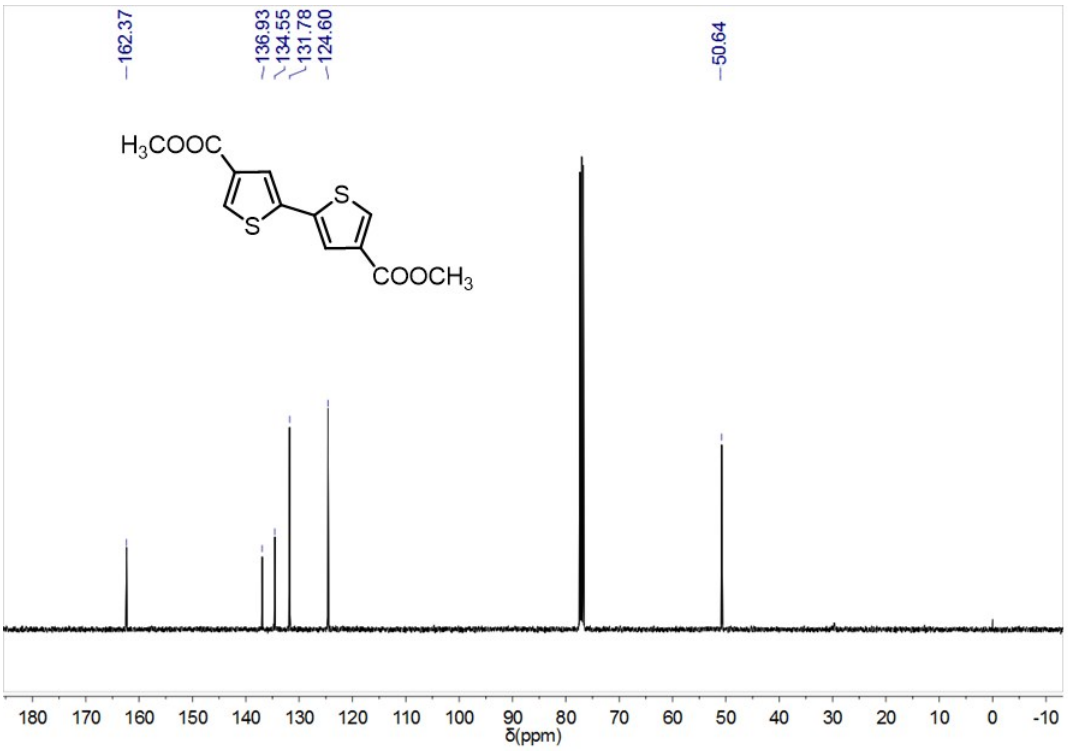

Fig. S3 ^{13}C NMR spectrum of compound **2a**.

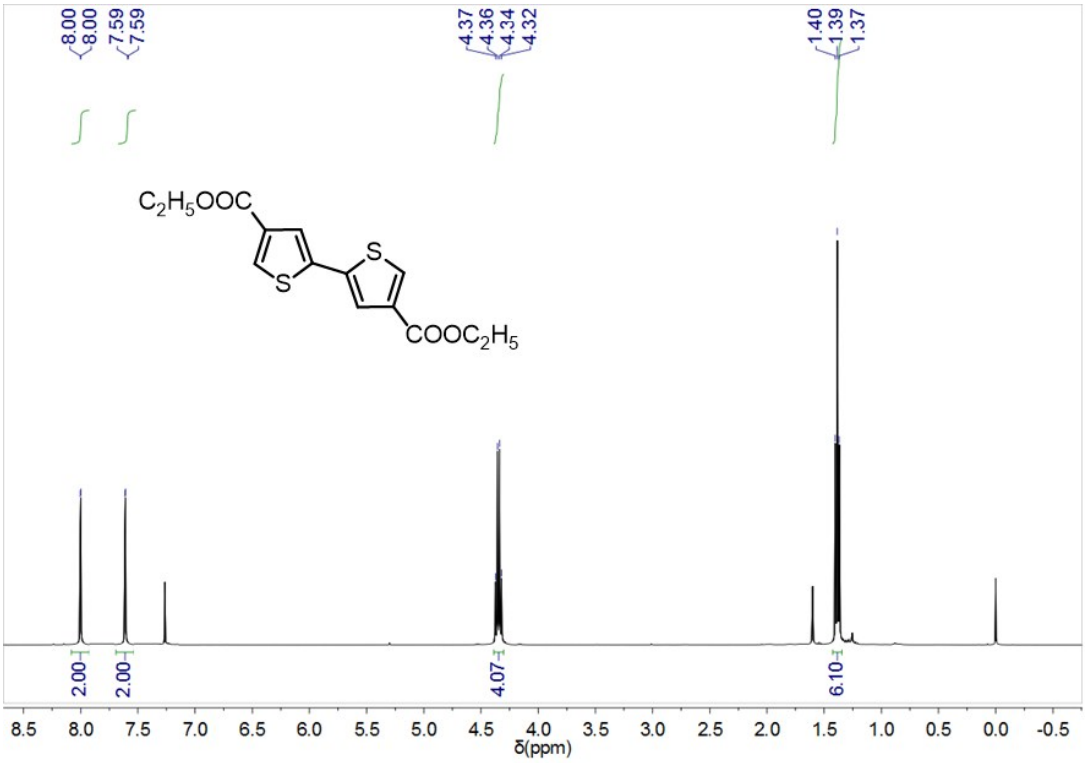

Fig. S4 ^{1}H NMR spectrum of compound **2b**.

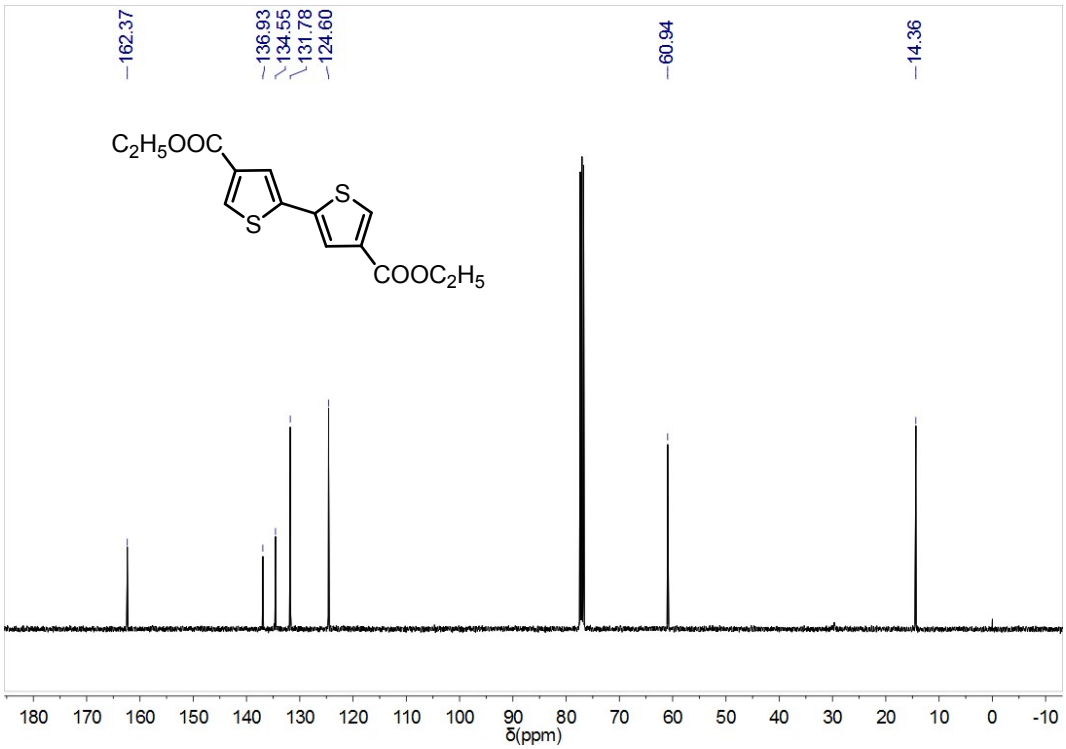

Fig. S5 ^{13}C NMR spectrum of compound **2b**.

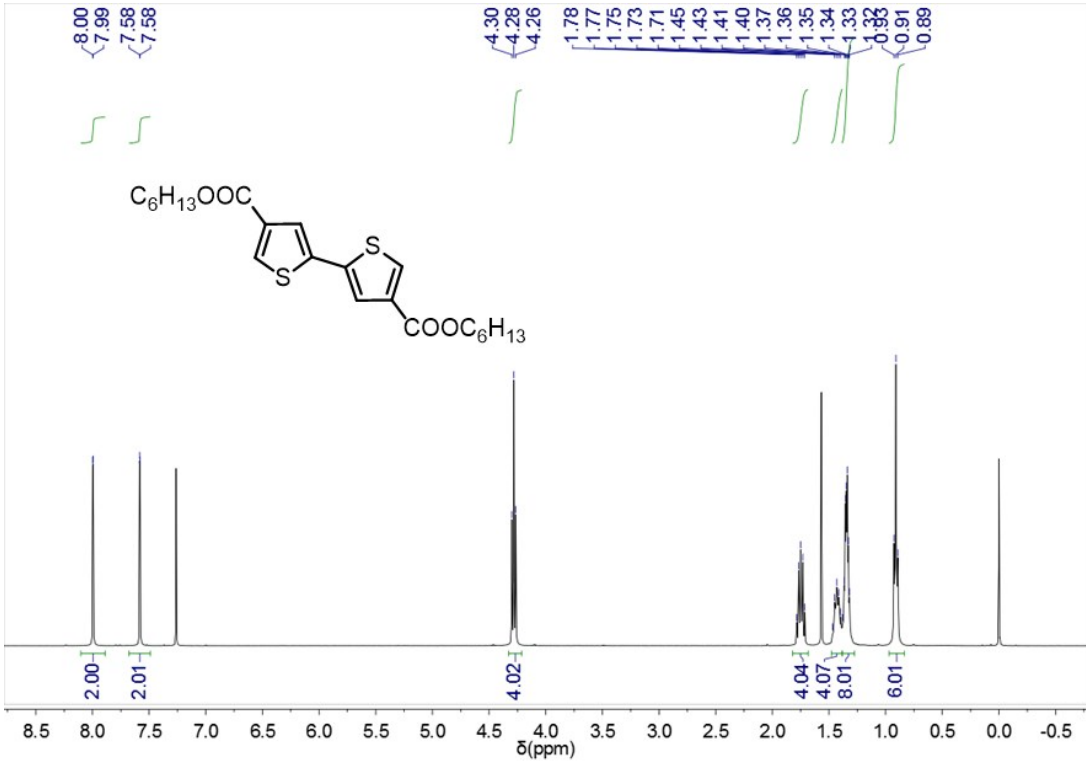

Fig. S6 ^{1}H NMR spectrum of compound **2c**.

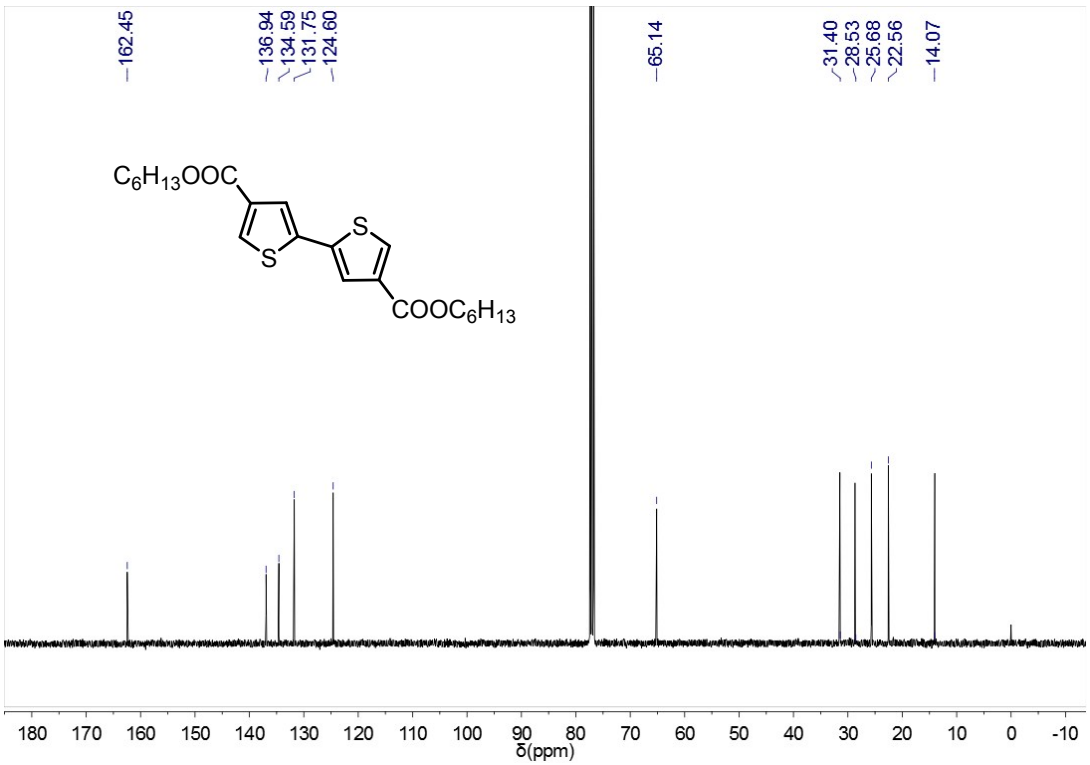

Fig. S7 ^{13}C NMR spectrum of compound **2c**.

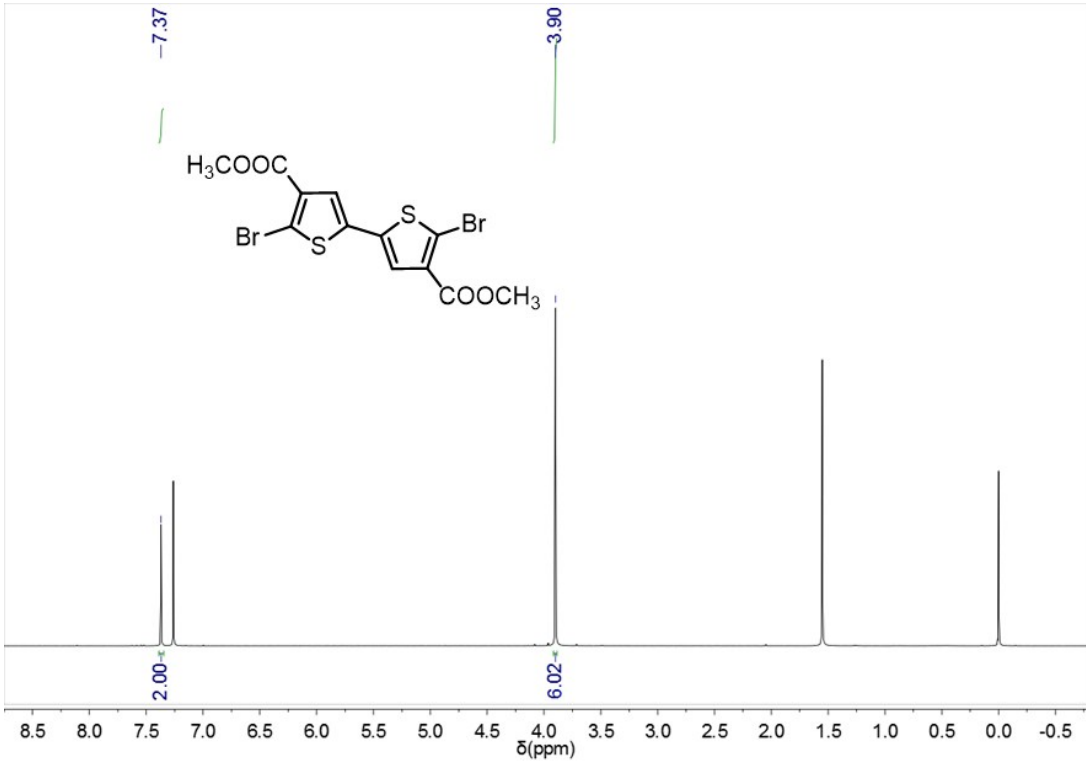

Fig. S8 ^{1}H NMR spectrum of compound **3a**.

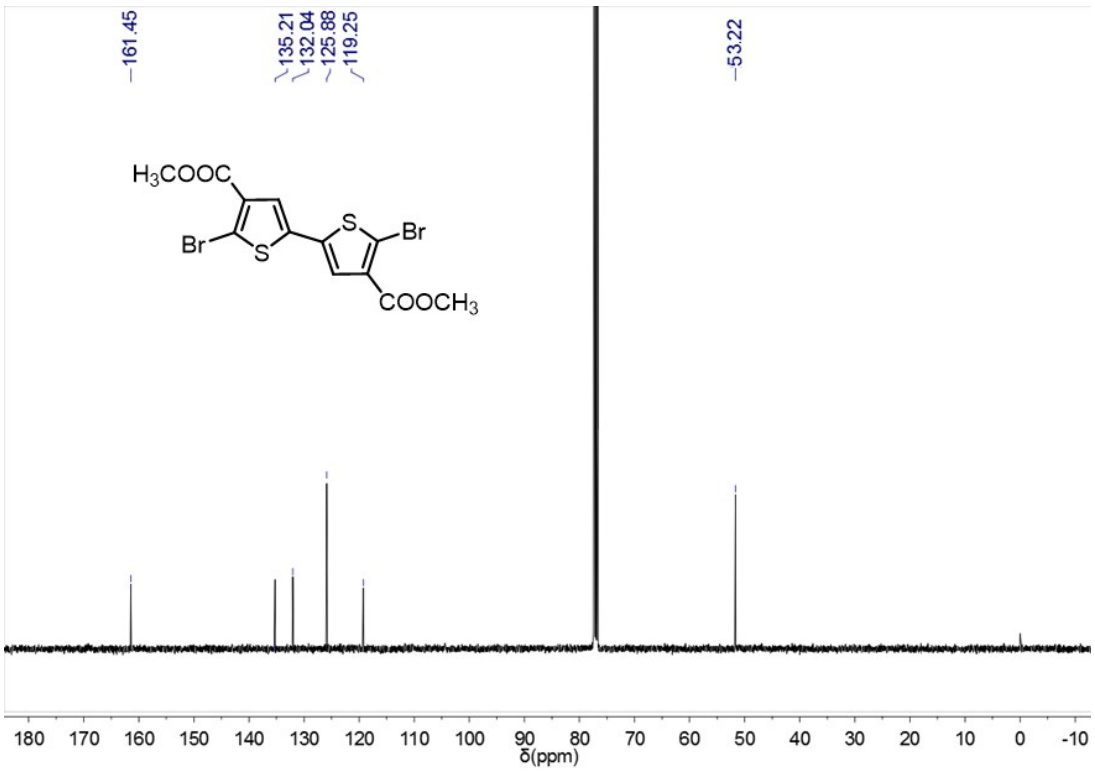

Fig. S9 ^{13}C NMR spectrum of compound **3a**.

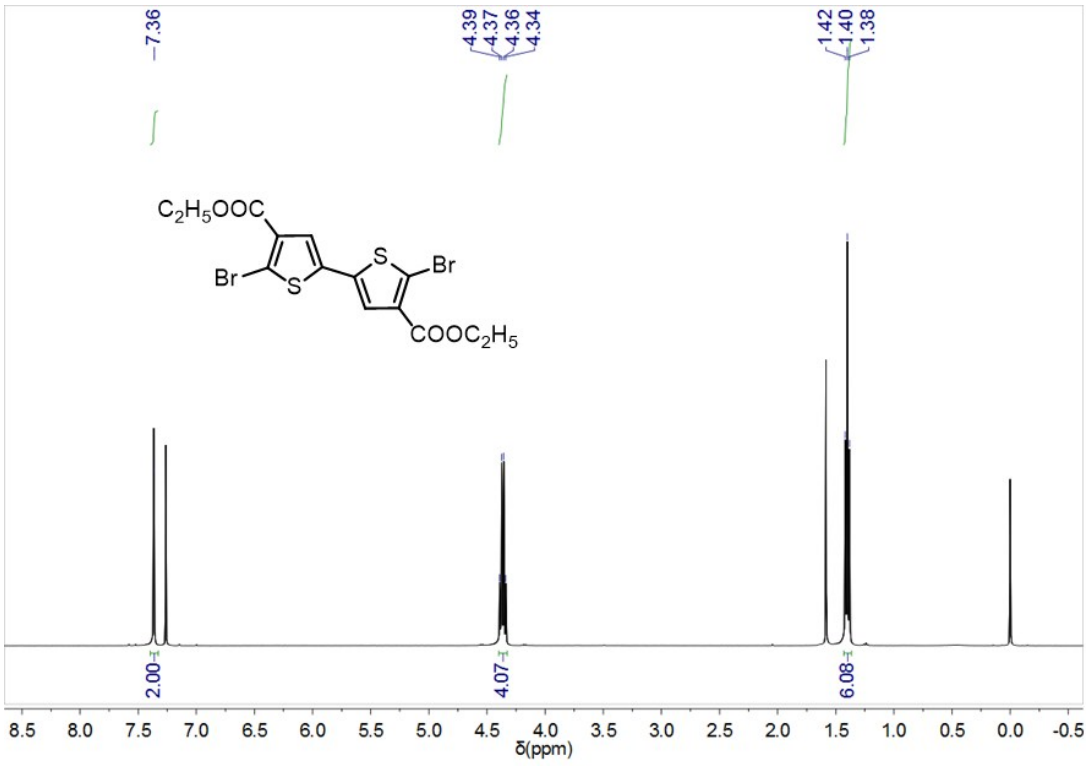

Fig. S10 ^{1}H NMR spectrum of compound **3b**.

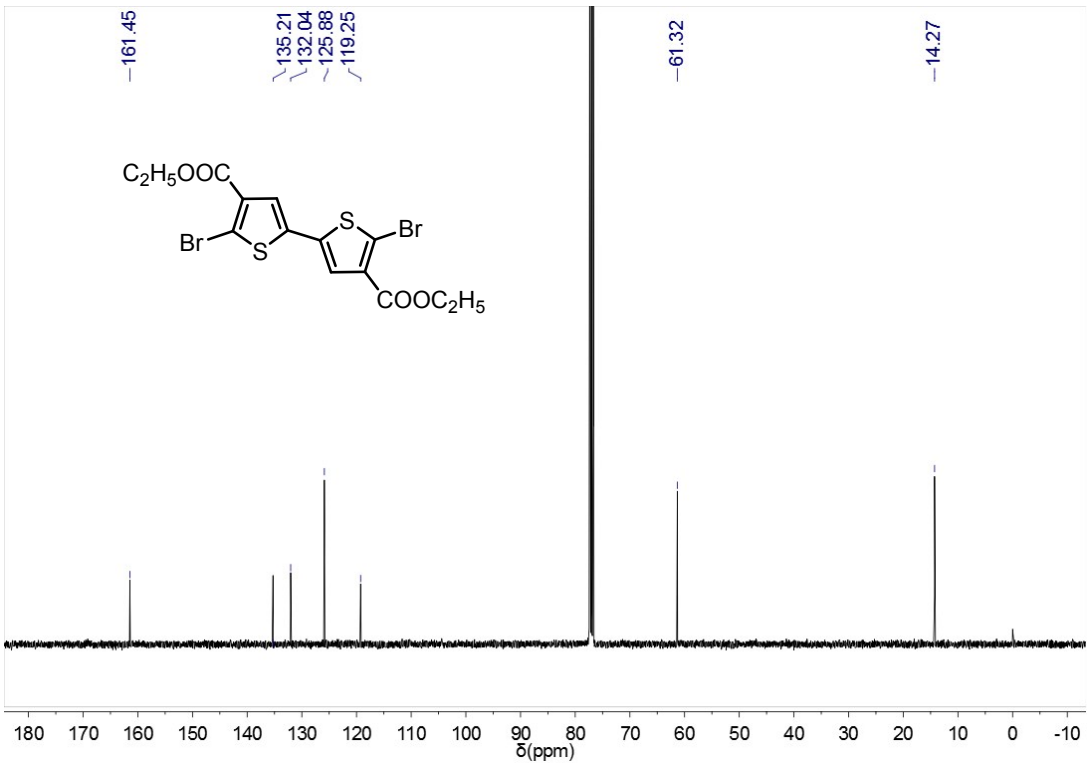

Fig. S11 ^{13}C NMR spectrum of compound **3b**.

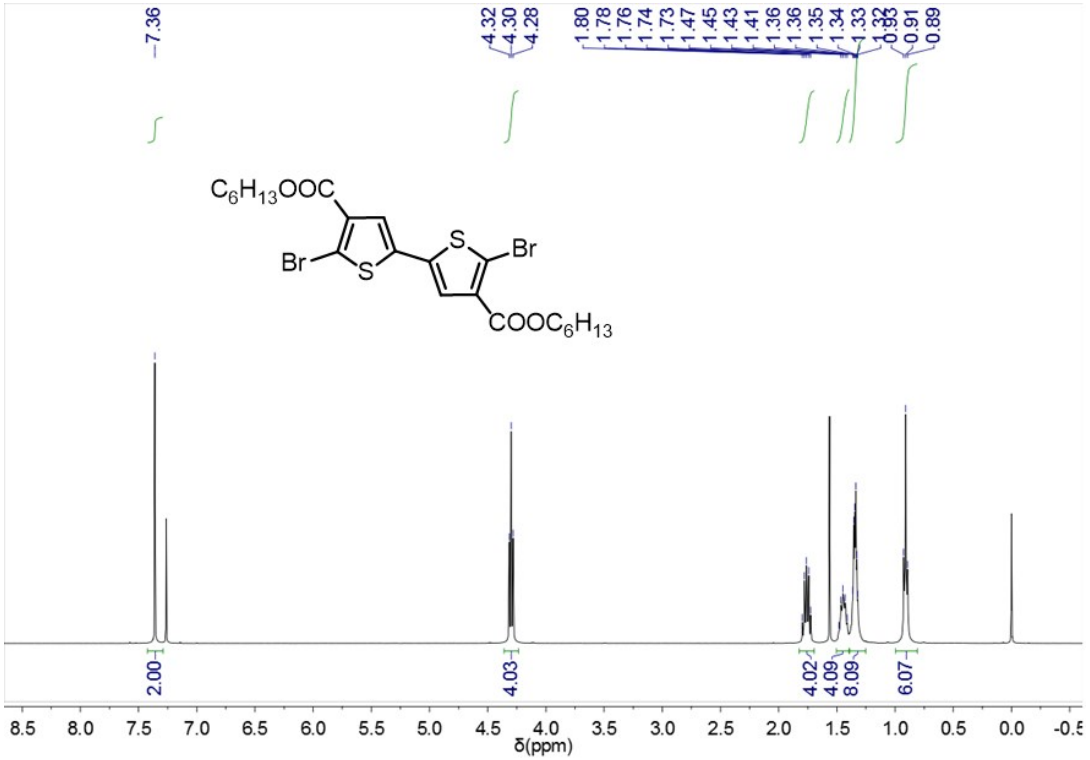

Fig. S12 ^{1}H NMR spectrum of compound **3c**.

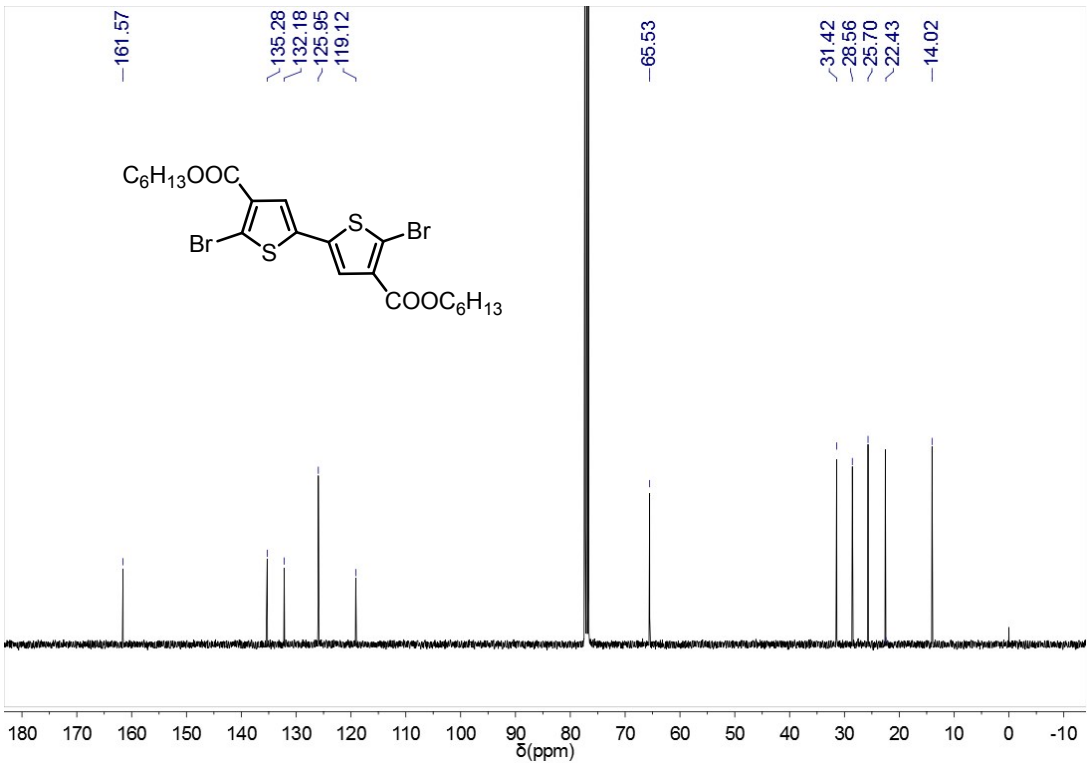

Fig. S13 ^{13}C NMR spectrum of compound **3c**.

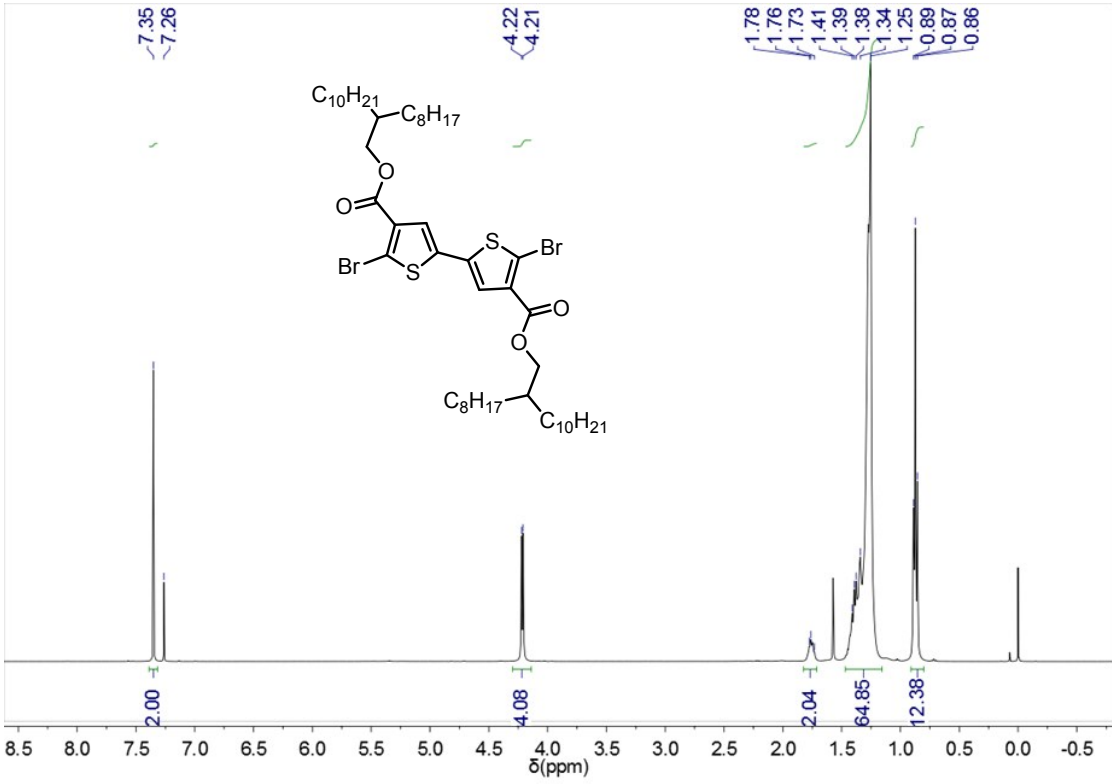

Fig. S14 ^{1}H NMR spectrum of compound **4**.

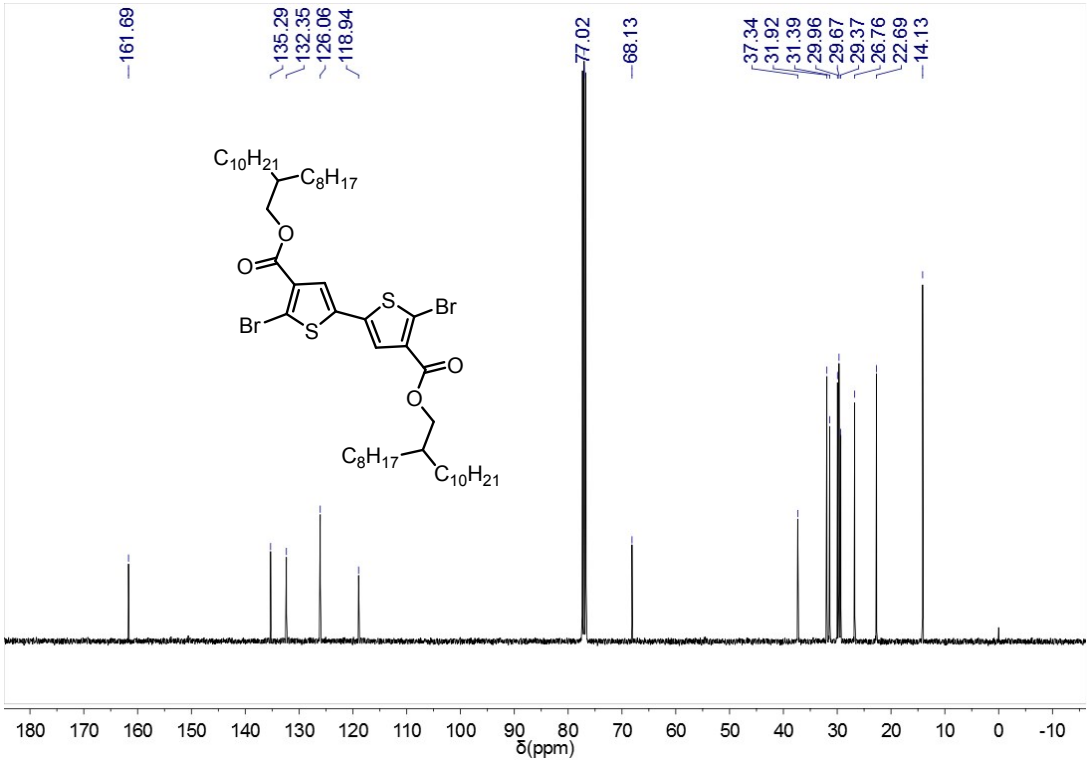

Fig. S15 ^{13}C NMR spectrum of compound **4**.

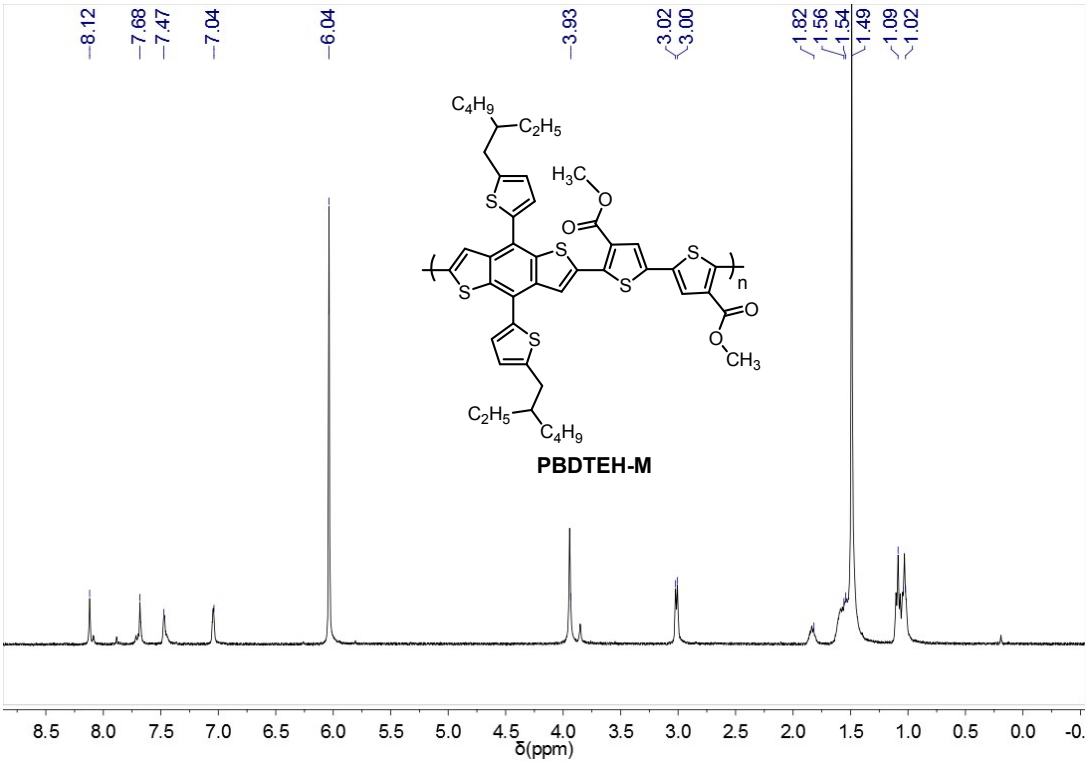

Fig. S16 ^{1}H NMR spectrum of **PBDTEH-M**.

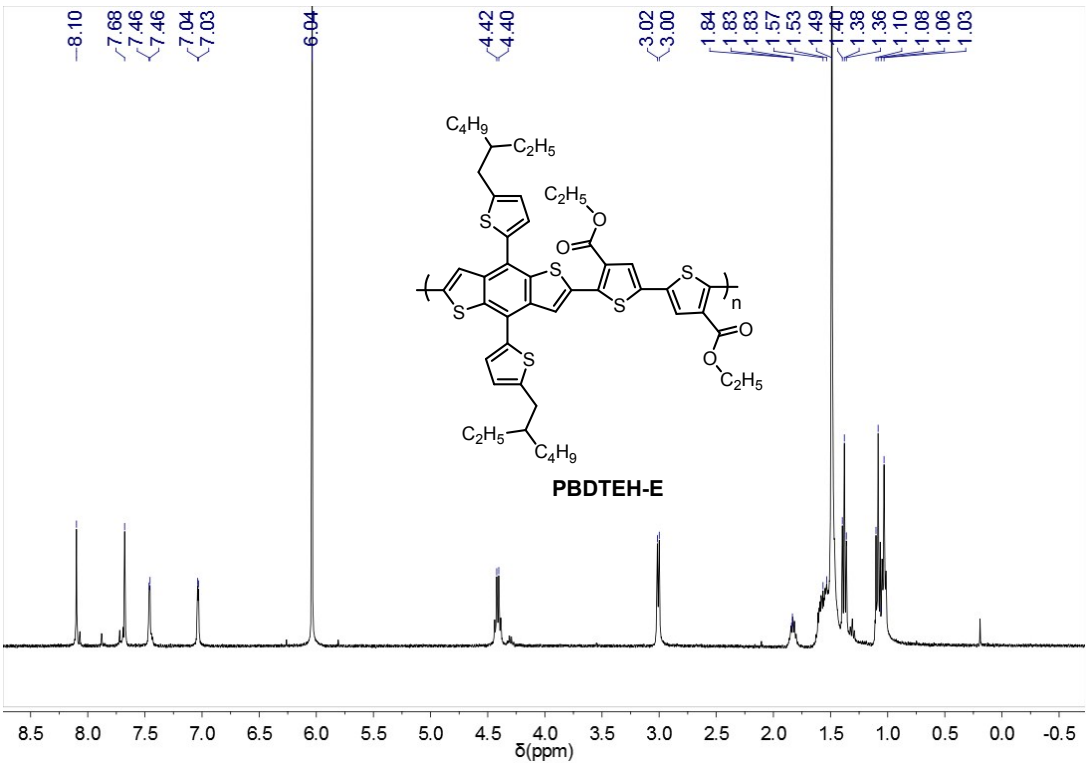

Fig. S17 ^{1}H NMR spectrum of **PBDTEH-E**.

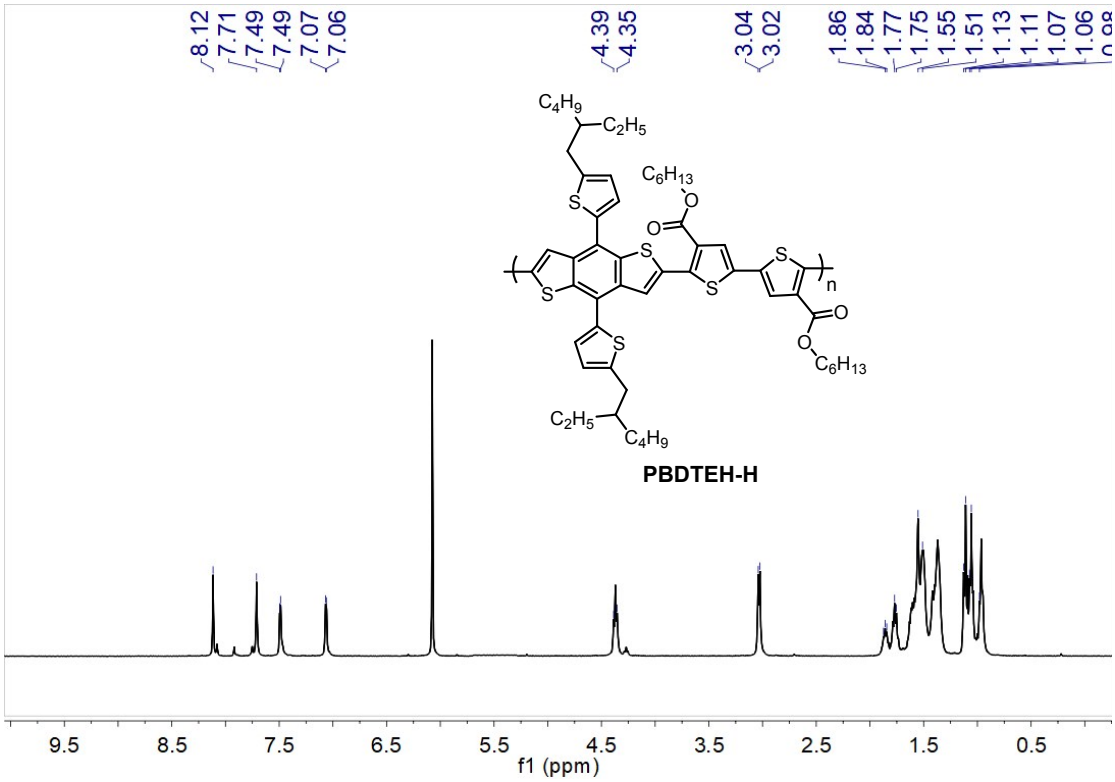

Fig. S18 ^{1}H NMR spectrum of **PBDTEH-H**.

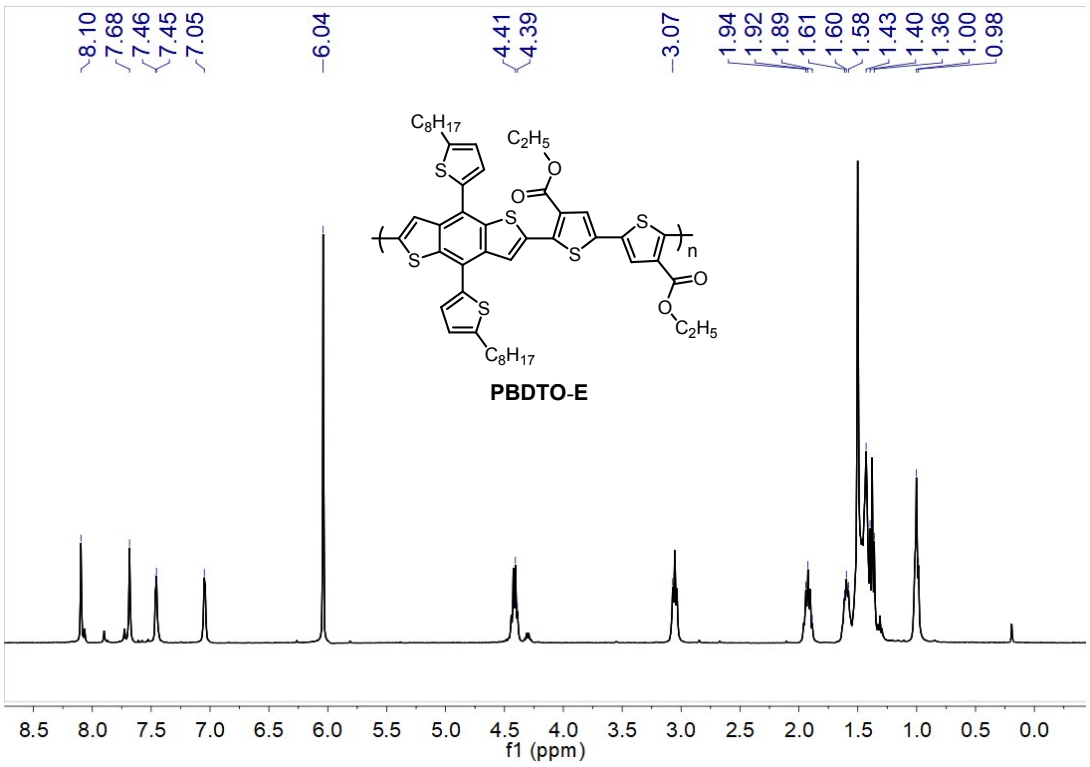

Fig. S19 ^{1}H NMR spectrum of **PBDTO-E**.

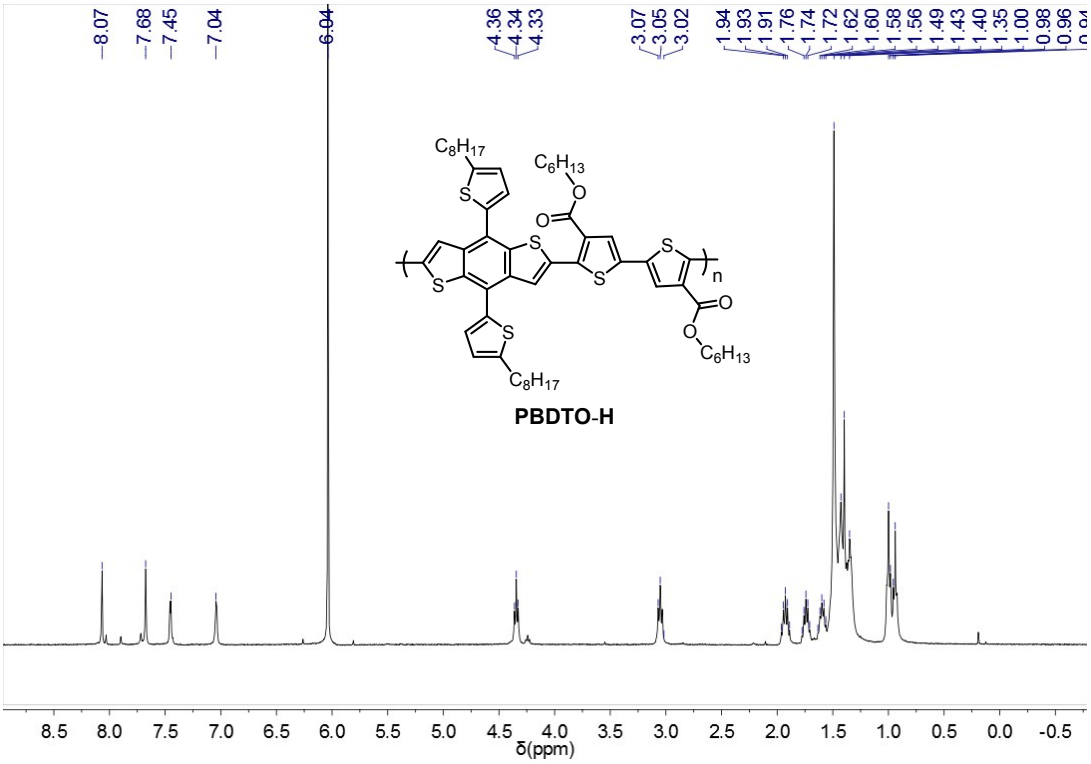

Fig. S20 ^{1}H NMR spectrum of **PBDTO-H**.

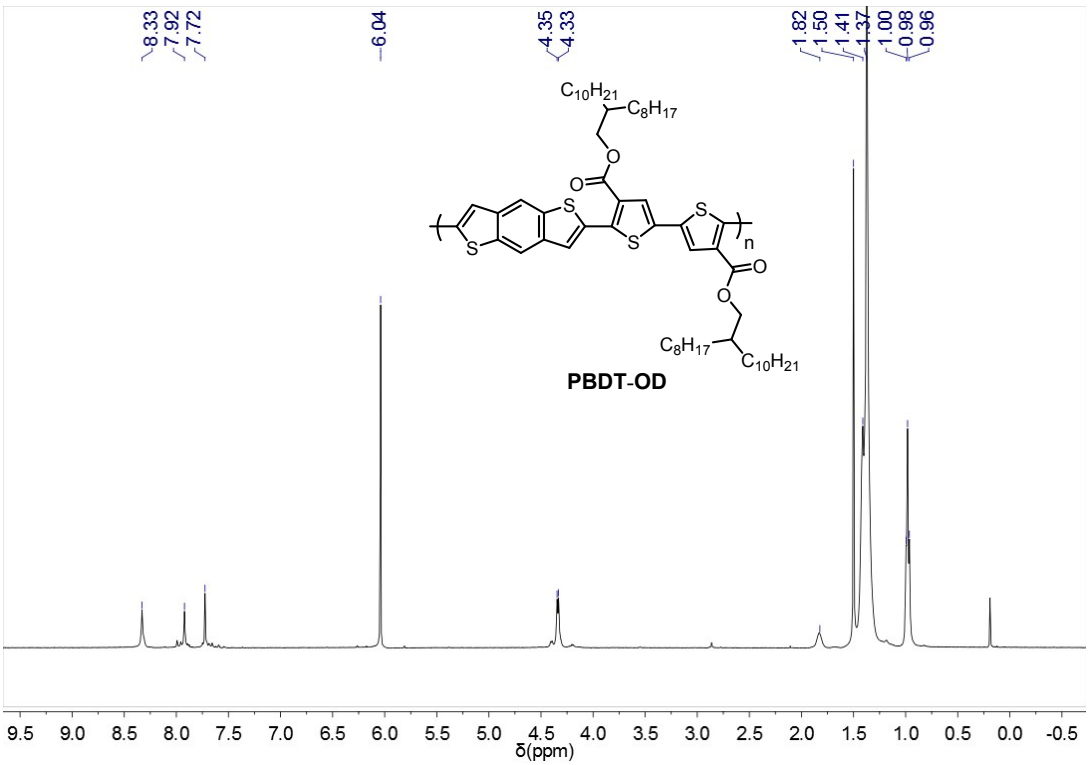

Fig. S21 ^{1}H NMR spectrum of **PBDT-OD**.

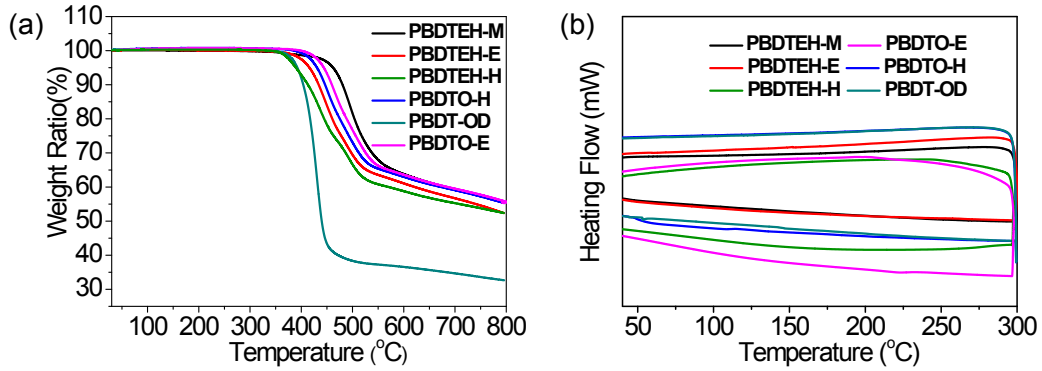

Fig. S22 TGA (a) and DSC (b) curves of the polymers.

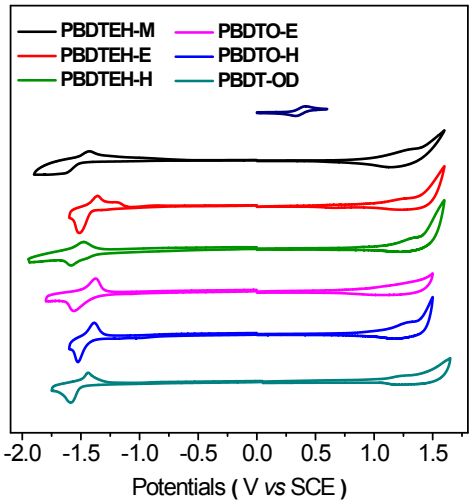

Fig. S23 Thin film cyclic voltammograms (CV) of the polymers.

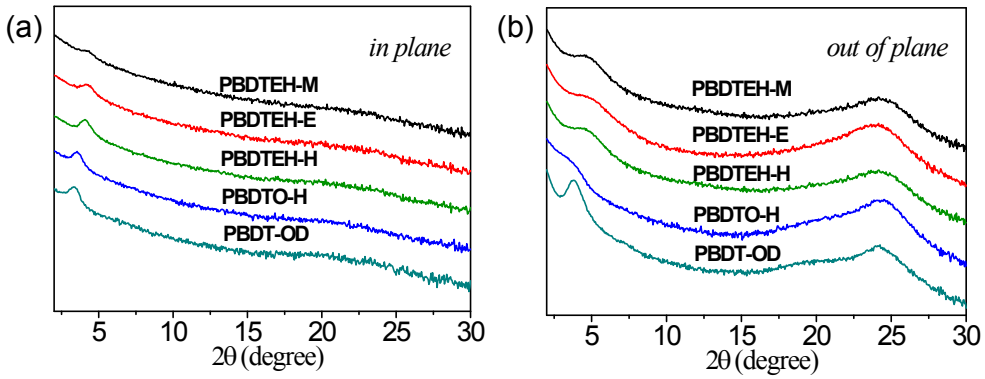

Fig. S24 In-plane (a) and out-of-plane (b) XRD patterns of the polymer neat films.

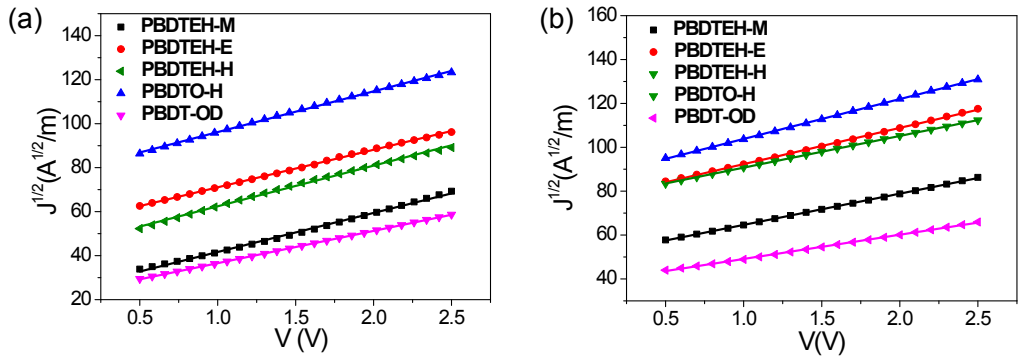

Fig. S25 *J-V* characteristics of hole-only devices based on the polymers. (a) for pristine films, (b) for films with thermal annealing at 150 °C for 10 min. Lines represent the fitting results using a model of single-carrier space-charge-limited current with field-independent mobility.

Table S1 Hole mobility of the polymer neat films measured by the space charge limited current (SCLC) method.

polymer	T_{anneal} (°C)	μ_{SCLC} (10^{-5} $cm^2V^{-1}s^{-1}$)
PBDTEH-M	Pristine	0.90±0.11 (1.04)
	150	1.58±0.10 (1.75)
PBDTEH-E	Pristine	0.99±0.10 (1.10)
	150	1.65±0.15 (1.82)
PBDTEH-H	Pristine	0.79±0.10 (0.90)
	150	1.55±0.14 (1.70)
PBDTO-H	Pristine	1.03±0.18 (1.29)
	150	2.40±0.15 (2.61)
PBDT-OD	Pristine	0.66±0.09 (0.79)
	150	0.82±0.10 (0.98)

[a] Optimal and statistical results are listed in parentheses and outside of parentheses, respectively. The average values are obtained from over 15 devices.

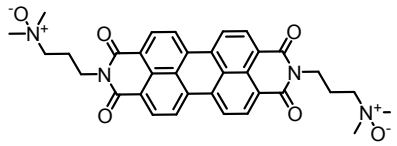

Fig. S26. Chemical structure of PDINO.

Table S2. Photovoltaic parameters of the PSC devices based on **PBDTEH-E**:ITIC-Th and **PBDTO-H**:ITIC-Th blend films with different D:A ratios (wt:wt).

polymer	D/A ratio	J_{sc} (mA/cm^2)	V_{oc} (V)	FF(%)	PCE(%)[c]
PBDTEH-E[a]	1:0.8	13.83	0.91	59%	7.19 (7.02)
	1:1	13.18	0.92	60%	7.43 (7.17)
	1:1.2	13.33	0.91	58%	7.05 (6.78)
PBDTO-H[b]	1:0.8	12.92	0.93	59%	6.99 (6.70)
	1:1	14.82	0.94	59%	8.21 (8.02)
	1:1.2	13.93	0.91	60%	7.74 (7.41)

[a] The blend solution was spin-coated from chlorobenzene with 0.2% DIO, and the blend film was annealed at 150 ^{o}C for 10 min.

[b] The blend solution was spin-coated from chlorobenzene with 0.2% DIO, and the blend film was annealed at 100 ^{o}C for 10 min.

[c] Optimal and statistical results are listed outside of parentheses and in parentheses, respectively. The average values are obtained from over 15 devices.

Table S3. Photovoltaic parameters of the PSC devices based on **PBDTEH-E**:ITIC-Th and **PBDTO-H**:ITIC-Th blend films with different active layer thicknesses.

polymer	thickness (nm)	J_{sc} (mA/cm^2)	V_{oc} (V)	FF(%)	PCE(%)[c]
PBDTEH-E[a]	80	10.31	0.91	53%	5.00 (4.75)
	100	13.18	0.92	60%	7.43 (7.17)
	120	14.13	0.89	52%	6.50 (6.28)
PBDTO-H[b]	80	13.25	0.93	53%	6.57 (6.31)
	100	14.82	0.94	59%	8.21 (8.02)
	120	14.69	0.94	56%	7.72 (7.33)

[a] The blend solution was spin-coated from chlorobenzene with 0.2% DIO, and the blend film was annealed at 150 ^{o}C for 10 min.

[b] The blend solution was spin-coated from chlorobenzene with 0.2% DIO, and the blend film was annealed at 100 ^{o}C for 10 min.

[c] Optimal and statistical results are listed outside of parentheses and in parentheses, respectively. The average values are obtained from over 15 devices.

Table S4. Photovoltaic parameters of PSC devices based on the polymer:ITIC-Th blend films with thermal annealing at different temperatures.

polymer	DIO (vol%)	Annealig temp.(°C)	J_{sc} (mA/cm^2)	V_{oc} (V)	FF(%)	PCE(%)[a]
PBDTEH-M	0	No	10.53	0.90	39%	3.75 (3.52)
	0	100	12.28	0.90	39%	4.32 (4.08)
	0	150	14.03	0.88	50%	6.16 (5.99)
	0	180	13.34	0.83	52%	5.80 (5.61)
PBDTEH-E	0.5	No	11.00	0.94	35%	3.65 (3.32)
	0.5	100	13.01	0.94	57%	6.96 (6.70)
	0.5	120	13.60	0.94	56%	7.18 (7.01)
	0.5	150	13.18	0.92	60%	7.43 (7.17)
	0.5	180	10.21	0.89	56%	5.14 (4.82)
PBDTEH-H	0.5	No	11.65	1.00	30%	3.31 (3.50)
	0.5	100	14.37	0.99	44%	6.20 (6.09)
	0.5	120	14.55	0.97	40%	5.35 (5.66)
PBDTO-H	0.5	No	11.18	0.96	39%	4.17 (3.88)
	0.5	80	12.55	0.95	45%	5.36 (5.09)
	0.5	100	14.82	0.94	59%	8.21 (8.02)
	0.5	120	14.66	0.94	53%	7.30 (7.05)
	0.5	150	12.67	0.93	60%	7.02 (6.75)
PBDT-OD	0	No	4.22	1.05	43%	1.88 (1.60)
	0	100	8.94	1.04	43%	4.03 (3.72)
	0	150	8.89	1.02	37%	3.40 (3.09)

[a] Optimal and statistical results are listed outside of parentheses and in parentheses, respectively. The average values are obtained from over 15 devices.

Table S5. Photovoltaic parameters of the PSC devices based on polymer:ITIC-Th blend films with different concentrations of DIO additive.

polymer	DIO (vol%)	Annealig temp.(°C)	J_{sc} (mA/cm^2)	V_{oc} (V)	FF(%)	PCE(%)[a]
PBDTEH-M	0	150	14.03	0.88	50%	6.16 (6.05)
	0.5	150	13.49	0.83	42%	4.67 (4.33)
PBDTEH-E	0	150	12.10	0.93	35%	3.89 (3.51)
	0.2	150	13.08	0.94	57%	6.99 (6.72)
	0.5	150	13.18	0.94	60%	7.43 (7.08)
	0.8	150	11.42	0.94	65%	6.90 (6.69)
	1	150	12.20	0.94	47%	5.36 (5.08)
PBDTO-H	0	100	11.18	0.96	39%	4.17 (3.94)
	0.2	100	11.56	0.94	57%	6.10 (5.81)
	0.5	100	14.82	0.94	59%	8.21 (8.02)
	0.8	100	14.92	0.94	54%	7.60 (7.25)
PBDTEH-H	0	100	10.99	1.01	32%	3.26 (3.55)
	0.5	100	14.37	0.99	44%	6.20 (6.09)
	1	100	13.00	0.97	35%	4.17 (4.41)
PBDT-OD	0	100	8.94	1.04	43%	4.03 (3.78)
	0.5	100	6.09	1.04	46%	2.90 (2.68)

[a] Optimal and statistical results are listed outside of parentheses and in parentheses, respectively. The average values are obtained from over 15 devices.

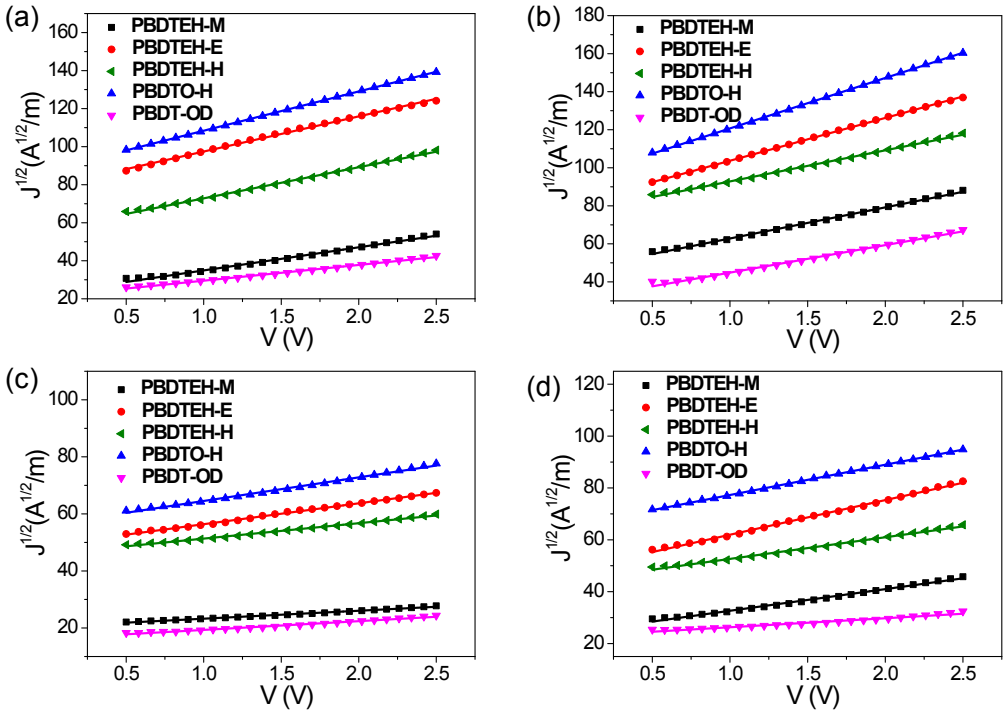

Fig. S27 *J-V* characteristics of hole-only (a, b) and electron-only (c, d) devices based on the polymer:ITIC-Th blend films: (a, c) for pristine blend films, (b, d) for blend films under optimized condition. Lines represent the fitting results using a model of single-carrier space-charge-limited current with field-independent mobility.

Table S6. Carrier mobility of the polymer:ITIC-Th blend films measured by SCLC method.

polymer	condition	μ_h (10^{-5} cm^2 V^{-1} s^{-1}) [a]	μ_e (10^{-5} cm^2 V^{-1} s^{-1}) [a]	μ_h/μ_e
PBDTEH-M	as cast	1.20±0.33 (1.56)	0.23±0.02 (0.26)	5.21
	TA [b]	9.32±0.11 (9.49)	1.83± 0.20 (2.11)	5.09
PBDTEH-E	as cast	3.15±0.13 (3.38)	0.86±0.14 (1.01)	3.66
	DIO [c]/TA [b]	8.45±0.35 (8.87)	2.43± 0.18 (2.62)	3.48
PBDTEH-H	as cast	2.50±0.23 (2.82)	0.56±0.08 (0.67)	4.21
	DIO [c]/TA [d]	7.15±0.22 (7.55)	1.67± 0.18 (1.90)	3.97
PBDTO-H	as cast	6.32±0.28 (6.65)	1.33± 0.08 (1.42)	4.75
	DIO [c]/TA [d]	11.90±0.87 (13.00)	3.60±0.15 (3.80)	3.30
PBDT-OD	as cast	1.05±0.14 (1.28)	0.18±0.03 (0.21)	5.83
	TA [d]	3.75± 0.25 (4.05)	1.03±0.17 (1.23)	3.64

[a] Optimal and statistical results are listed in parentheses and outside of parentheses, respectively. The average values are obtained from over 15 devices. [b] The thermal annealing temperature is 150 °C. [c] The DIO concentration is 0.5% (vol%). [d] The thermal annealing temperature is 100 °C

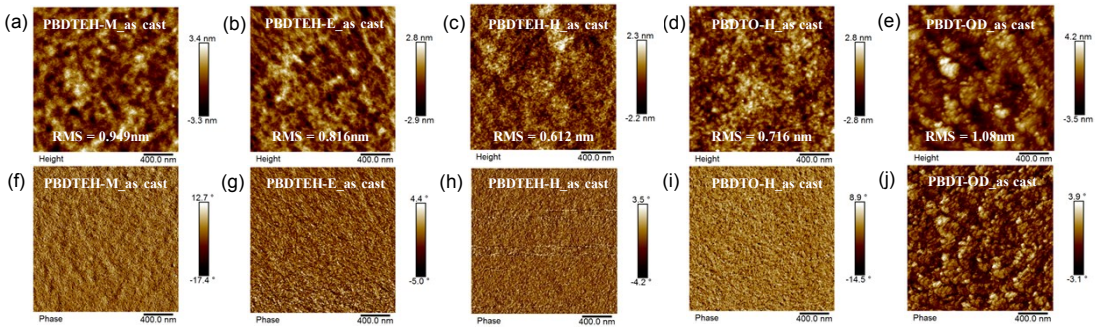

Fig. S28 AFM height (a-e) and phase (f-j) images of the polymer:ITIC-Th blend films without any post treatment.

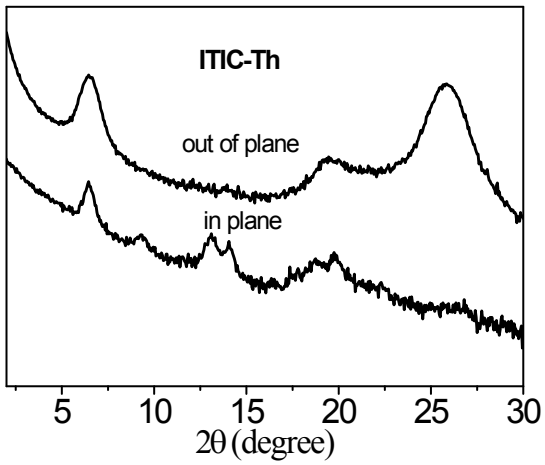

Fig. S29 In-plane and out-of-plane XRD patterns of ITIC-Th neat film with thermal annealing at 150 °C for 10 min.